LIMNOLOGY
and
OCEANOGRAPHY: METHODS

ASLO

Limnol. Oceanogr.: Methods 2026, e70031

doi: 10.1002/lom3.70031

EVALUATIONS OF EXISTING METHODS

Comparing non-staining methods with Mutvei's solution to visualize growth increments in short-lived intertidal marine gastropod shells

Mahsa Alidoostsalimi,[1,2]* Amy L. Prendergast,[1,2]* Sean Ulm,[2,3] Ariana B. J. Lambrides,[2,3] Ian J. McNiven,[3,4] Russell N. Drysdale,[1] Nguurruumungu Indigenous Corporation,[5] and Walmbaar Aboriginal Corporation RNTBC[6]

[1]ARC Centre of Excellence for Indigenous and Environmental Histories and Futures, School of Geography, Earth and Atmospheric Sciences, University of Melbourne, Melbourne, Victoria, Australia; [2]ARC Centre of Excellence for Australian Biodiversity and Heritage, College of Arts, Society and Education, James Cook University, Cairns, Queensland, Australia; [3]ARC Centre of Excellence for Indigenous and Environmental Histories and Futures, James Cook University, Cairns, Queensland, Australia; [4]ARC Centre of Excellence for Australian Biodiversity and Heritage, Monash Indigenous Studies Centre, Monash University, Clayton, Victoria, Australia; [5]Nguurruumungu Indigenous Corporation, PO Box 886, Cooktown, Queensland, Australia; [6]Walmbaar Aboriginal Corporation RNTBC, Hope Vale, Queensland, Australia

Abstract

Mutvei's solution is a widely utilized standard staining method for revealing growth increments in biogenic carbonates; however, it is a slightly toxic, destructive approach with varying success across species groups. Therefore, there has been growing interest in finding non-toxic, less destructive, and straightforward alternative techniques for studying growth structures, primarily focusing on long-lived shells. This research focuses on an intertidal short-lived marine gastropod—*Conomurex luhuanus*, collected from the Great Barrier Reef and a nearby archaeological site. A comparative analysis of common and cost-effective tools used for growth increment visualization—including transmitted-light microscopy, reflected-light microscopy, cathodoluminescence, Raman spectroscopy, and acetate peel against Mutvei's solution—was undertaken to determine the most effective method to visualize daily growth increments in *C. luhuanus*. Overall, our results suggested that the relative patterns of measuring growth increments using all techniques are broadly consistent ($r = 0.4$–0.7, $p < 0.05$) in the absence of slowed or halted growth. However, transmitted-light microscopy (TML) was the only method that revealed more growth increments in an area where growth lines were too thin to be detected using other techniques, making it impossible to distinguish the daily growth increments using those techniques. Transmitted-light microscopy, without staining or thin-sectioning, was an effective and time-efficient technique for visualizing daily growth increments in *C. luhuanus*. We suggest that TML can be considered as a preliminary step to investigate growth increments in other species before applying established approaches, such as Mutvei's solution.

Marine calcifying organisms, particularly bivalve and gastropod mollusks, can record a plethora of chronologically constrained information within their successive increments of biogenic carbonate growth. This information is encoded via multiple physical and geochemical proxies (e.g., oxygen isotopes and trace elements) through the life history of the organism and can be divided into three main categories: (1) climate and environmental information; (2) life history traits and ecology; and (3) people-environment interactions (Berry and Barker 1968; Carré et al. 2005; Schöne et al. 2007; Andrus 2011; Twaddle et al. 2016; Patterson et al. 2010; Nishida et al 2026; Prendergast et al. 2016; Surge and Barrett 2012; Walliser and

*Correspondence: mahsa.alidoostsalimi@student.unimelb.edu.au, amy.prendergast@unimelb.edu.au

Associate editor: Kozue Nishida (GE)

Schöne 2020). Marine shells have the potential to record this information at annual to sub-daily resolution owing to their continuous growth—despite the possibility of growth interruption in many genera due to environmental and vital effects (Fenger et al. 2007; Butler and Schöne 2017; Twaddle et al. 2017; Hollyman et al. 2020; Alidoostsalimi et al. 2025). This breadth of information and temporal resolution is not typically achievable from many other commonly used palaeoenvironmental archives, such as sediment and ice cores, making mollusk shells a valuable environmental archive for many different disciplines (e.g., palaeoceanography, palaeoecology, and archaeology). Sclerochronology—analogous to dendrochronology—allows us to decipher the meaning of these physical characteristics and biogeochemical parameters within growth increments (GIs) (Oschmann 2009; Butler and Schöne 2017).

The underlying basis of all sclerochronology is the study of incremental growth patterns to understand what resolution—annual to sub-daily information—can be obtained from these biogenic archives. Such information is critical as it enables sclerochronologists to estimate the duration represented in each growth increment, which in turn is required for accurately interpreting time series of proxy data collected from these growth increments (Schöne et al. 2005; Beierlein et al. 2015). Two established methods, acetate peel and Mutvei's solution, have been commonly used to reveal and enhance growth increments in shell sclerochronology (Ropes 1984, 1987; Schöne et al. 2005). Mutvei's solution is a standard staining method to enhance the visibility of growth increments (GIs) and is remarkably effective in visualizing GIs in a wide range of biological carbonates (Schöne et al. 2005). However, Mutvei's solution is slightly physically destructive due to the etching of the surface and contains glutaraldehyde, a respiratory toxin component (Schöne et al. 2005; Wanamaker et al. 2009; Sigma-Aldrich 2023). While few studies have suggested that this solution does not significantly affect the biogeochemical properties of carbonate shells, its impact on isotopes may differ across different specimens (various microstructures and types of shell organic matrix) (Schöne et al. 2017). Additionally, the success of this method in visualizing incremental growth patterns is variable from species to species. It is influenced by the concentration of polysaccharides and other organic compounds because the contrast provided through staining is related to the amount of polysaccharides in shell structures (Schöne et al. 2005; Welsh et al. 2011). This inherent variability highlights that not all well-established techniques are suitable for visualizing growth increments in every species. Therefore, unsuccessful results pave the way to explore less destructive, less toxic, and time-saving alternative methods that can provide more detailed and less unambiguous depictions of growth increments (Table 1; Wanamaker et al. 2009; Karney et al. 2011; Welsh et al. 2011; Barbin 2013; Beierlein et al. 2015; Yan et al. 2020)

Many previous studies have focused on visualizing growth increments in long-lived marine bivalve shells (lifespan > 12 yr) (e.g., *Arctica islandica* and *Tridacna* spp.) by virtue of their potential to establish long-term records of environmental changes at sub-annual to daily resolutions (Gosling 2008; Wanamaker et al. 2009; Karney et al. 2011; Beierlein et al. 2015; Yan et al. 2020; Liu et al. 2022). However, less attention has been paid to visualizing growth increments in intertidal short-lived marine mollusks (lifespan < 3 yr) (Gosling 2008), particularly marine gastropod shells. Meanwhile, they have the potential to provide similar information with several additional advantages.

Marine gastropod shells are one of the most common intertidal marine faunal components found in modern coastal ecosystems as well as forming a significant component of coastal shell middens (Álvarez et al. 2011; Andrus 2011; Colonese et al. 2011; Giovas 2016; Hollyman et al. 2018; Lambrides et al. 2020; Rick 2023). Biogeochemical properties in shells' carbonate serve as an invaluable proxy, offering critical insights into people-environment interactions, including shellfish harvesting practices and archaeological site occupation. Additionally, they have the potential to provide high-temporal resolution records at sub-annual to sub-daily scales, aiding in reconstructing coastal palaeotemperatures and other paleoclimate parameters (e.g., sea surface temperature, salinity, and nutrient availability) in their growth structures and geochemistry (Ekaratne and Crisp 1982; Fenger et al. 2007; Schöne et al. 2007; Mannino et al. 2008; Radermacher et al. 2009; Gutiérrez-Zugasti et al. 2015; Prendergast et al. 2016; Prendergast and Schöne 2017; Hausmann et al. 2017; García-Escárzaga et al. 2020; Gutiérrez-Zugasti 2025; Alidoostsalimi et al. 2025). Their potential to generate high-resolution data allows them to serve as archives of climate dynamics. In some regions where there is a paucity of long-lived biological archives (e.g., Peru), chemical proxies obtained from intertidal archaeological short-lived marine shells have been used as a biogeochemical repository to reconstruct Holocene ENSO (El Niño Southern Oscillation) at high-resolution. Additionally, they have the potential to be used to address uncertainties in climate models (Carré et al. 2005, 2013; Etayo-Cadavid et al. 2013; Warner et al. 2022).

Although some alternative methods, such as transmitted-light microscopy, acetate peels, and a combination of SEM and etching, have been individually used to recognize growth increments (Ekaratne and Crisp 1982; Tojo and Ohno 1999; Schöne et al. 2005; Fenger et al. 2007; Hausmann et al. 2017; Wang et al. 2012), there has been no comprehensive comparison between methods useful for short-lived intertidal marine gastropod shells. For the first time, we aim to apply different methods for imaging lunar-tidal daily growth increments in a short-lived marine gastropod, *Conomurex luhuanus*. *C. luhuanus*, used in this short study, is the primary species for oxygen isotope analysis (Alidoostsalimi et al. 2025). We were unable to easily visualize and distinguish growth increments from one another using Mutvei's solution, particularly in parts where the shells show slow growth. To address this, we conducted a short comparative analysis using some of the most common and cost-effective analytical tools available in

Table 1. An overview of methods used to enhance and visualize growth increments in previous sclerochronology studies of mollusk and other biogenic materials.

Technique	Preparation	Biological carbonates	Destructive	References
Acetate peel	Chemical pretreatment	Shells	Yes	Ropes 1984, 1987
Etching technique	Chemical pretreatment	Shells and corals	Yes	Risk and Pearce 1992; Schöne et al. 2005
Scanning electron microscopy (SEM) with etching	Thin section and sometimes coating the surface for SEM Chemical pretreatment	Shells	Yes	Tojo and Ohno 1999; Schöne et al. 2005
0.5% Rhodamine B solution	Chemical pretreatment Thin section (30–50 μm)	Long-lived bivalve shells	Yes	Schöne et al. 2002
Mutvei's solution	Chemical pretreatment	A range of biogenic carbonates	Yes	Schöne et al. 2005
Calcein staining method	Chemical pretreatment	Gastropod shells	Yes	Guzman et al. 2007
Fluorescence microscopy	No	Long-lived bivalve shells Gastropod shells	No	Guzman et al. 2007; Wanamaker et al. 2009; Liu et al. 2022
Backscattered electron microscopy (BSE)	No	Long-lived bivalve shells		Karney et al. 2011
Transmitted light without a thin section	Thickness (1 mm or 7 mm)	Long-lived bivalve shells Gastropod shells	No	Welsh et al. 2011; Wang et al. 2012; Burchell et al. 2013
Cathodoluminescence microscopy (CL)	No	Shells	No	Barbin 2013
Raman spectroscopy	No	Long-lived bivalve shells	No	Beierlein et al. 2015
Laser scanning confocal microscope (LSCM) (autofluorescence microimage)	No	Long-lived bivalve shells	No	Yan et al. 2020
Transmitted light with etching or thin section	Thin section (e.g., $\sim$ 60 μm) and chemical pretreatment	Long-lived bivalve shells Freshwater shells	No	Schöne 2008; Burchell et al. 2018; Mills et al. 2023

Earth Science and Geography departments, including Confocal Raman microscopy, transmitted-light microscopy, cathodoluminescence, reflected-light stereomicroscopy, and acetate peels. These approaches were compared against Mutvei's solution to determine which method provides the clearest image, allowing us to effectively, quickly, and easily distinguish successive growth increments in *C. luhuanus*. The results obtained from this short study assist sclerochronologists in considering other methods to visualize growth increments when established techniques fail to provide a clear image of growth increments, especially in areas where the shells experience slower growth.

Materials and procedures

Samples

Conomurex luhuanus (Linnaeus, 1758; family: Strombidae)—previously known as *Strombus luhuanus*—is a medium-sized shell (maximum length 60 mm) that lives in intertidal reef flats across the western Indo-Pacific. This short-lived marine gastropod (suggested to live up to 3 yr) is a valuable fisheries resource for coastal communities (Catterall and Poiner 1983). It is one of the most commonly excavated species from coastal archaeological shell middens in the Great Barrier Reef and other Pacific regions (Takamiya 2006; Ulm et al. 2019; Faulkner et al. 2020; Lambrides et al. 2020). Strombidae shells are composed of aragonite, and some genera have been successfully used as archives to study paleoenvironment and people-environment interactions (Cornu et al. 1993; Radermacher et al. 2009; Hausmann et al. 2017; Alidoostsalimi et al. 2025). For this study, live samples were collected during the southern hemisphere cold season (August) in 2019 and 2023 from the intertidal reef flat (for more details on sampling, *see* Alidoostsalimi et al. 2025), and the archaeological samples were excavated from a Holocene shell midden (South Island Headland Midden, SIHM), both sample sets from South Island, Jiigurru (Lizard Island Group), the Great Barrier Reef

(Supporting Information Fig. S1). The archaeological samples were not directly dated; however, they were recovered from an excavation unit at SIHM, which has been dated to approximately 1000–3000 yr ago (for more details, *see* Ulm et al. 2024).

Sample preparation

Conomurex luhuanus has a conical and medium-sized shell. A lip, which is the thickest part of the shell, is the area where growth increments can most easily be visualized in Strombidae shell sections and can be used for sectioning (Figs. 1, 2) To prevent any breakage while cutting the shells, the surface of the specimens was painted using metal epoxy resin (JB Kwik Weld). Specimens were sectioned perpendicular to the maximum growth axis using a Buehler Isomet 1000 Precision low-speed saw equipped with a 0.4 mm thick diamond-edged blade. For each specimen, two slices with a thickness of 2–3 mm each were obtained—the common thickness usually used for sclerochronology. Afterward, the slides were manually ground using 2000, 3000, and 5000 grit paper and then polished using 1-μm aluminum oxide powder in suspension on a Buehler polishing cloth to have a smooth surface where we could observe the growth increments.

Experimental design

This research focuses on investigating which method effectively and straightforwardly distinguishes successive growth increments (GIs), particularly in areas where GIs were hardly distinguishable using reflected stereomicroscopy and Mutvei's solution. A growth increment is characterized as the whole growth occurring between two growth lines (GLs) and is formed during a defined time period (sub-daily to annually). Without observing growth lines, distinguishing GIs may not be possible.

To compare growth increment visibility using the different methods, images obtained from stained sections (Mutvei's solution) were considered as a control group. The effectiveness and quality of the other methods in visualizing and distinguishing successive GIs were compared against this control. To ensure consistency in investigating the same successive GIs, the same shell section was used for all analyses on a specimen whenever possible; however, in a few cases a mirrored section (from the same shell) was used as the original shell section was used for oxygen isotope analysis (Table 2). Within each shell section, we selected an area that was easily distinguishable and detectable based on features in the shell's architecture. We used different techniques to visualize this same area. We chose to focus on an area where some growth increments (GIs) could not be easily distinguished under reflected-light stereomicroscopy to see whether other techniques might enhance visibility of GIs. For the selected area, we counted the number of growth increments and measured the widths of successive growth increments using images obtained from each different technique. Counting the number of growth increments was conducted on digital photos, and measuring the width of growth increments was done using ImageJ 1.53t (Java 1.8.0-345, 64-bit). Multiple correlations along with Cronbach's alpha and the intraclass correlation coefficient (ICC2) were performed using Python software (version 3.8.8) to examine the statistical difference between GI observations. We have provided Python scripts in a public GitHub repository (https://github.com/MahsaAS86/Correlation_Heatmap_Growth_Increments). These scripts serve as a template for others to test and visualize their data, similar to the approach we presented in Fig. 4.

Analyzing growth increments

We selected four modern and four archaeological shells (Table 2). First, the shells' lips were investigated using reflected stereomicroscopy (RM) (Leica M80, 50× with a Leica IC90 E0 camera), transmitted-light microscopy (TML) (Zeiss AxioImager M1m microscope, 5–10×, with IDS 3370CP-C-HQ camera), and cathodoluminescence microscopy (CL). Under TML, the light passes through the cross-sectioned shells to the opposite side of the specimens toward the objective lens, while in RM, the light illuminates the samples from above. Cathodoluminescence microscopywas carried out on a Nuclide ELM2B Cathodoluminoscope attached to a Wild M400 Photomacroscope operating at 8–10 kV with a 0.6 milliamp beam current and photographed using a Q-imaging Micropublisher 6 cooled CCD camera (20–25×). We qualitatively observed narrow and wide growth increments across the entire shell lip and visually compared which method more clearly and more easily distinguishes successive growth increments (Supporting Information Figs. S2, S3). Additionally, we counted the number of growth increments in a defined area (Table 2). Our observations indicated that images obtained through TML were clear and provided more detailed growth increment patterns, regardless of whether the shells were modern or archaeological (Supporting Information Figs. S2, S3; Table 2). Therefore, within the samples, we selected two modern (SI30-C1-4 and C-13) and two archaeological (FS26-XU10-4 and FS93-XU36-9) sections for applying other methods and comparing with Mutvei's solution.

Two modern (SI30-C1-4 and C-13) and two archaeological (FS26-XU10-4 and FS93-XU36-9) sections were investigated using Confocal Raman Microspectroscopy (CRM). Confocal Raman Microspectroscopy is a non-destructive method, which can be used to identify the mineralogy of the shells. Confocal Raman Microspectroscopy is equipped with a standard optical microscope, allowing high-magnification visualization of a sample, with the advantage of investigating the chemical characteristics (aragonite and calcite) of the shells simultaneously. Shell sections were examined by Renishaw Raman Spectroscopy (Renishaw Centrus 1C4A75) with a 50× long working distance objective in a confocal mode at the Materials Characterization and Fabrication Platform (MCFP), the University of Melbourne. A 785 nm laser at a maximum power of 100 mW was used for acquiring spectra. Raman emission was observed using a grating with 1200 lines mm^{-1}. We used

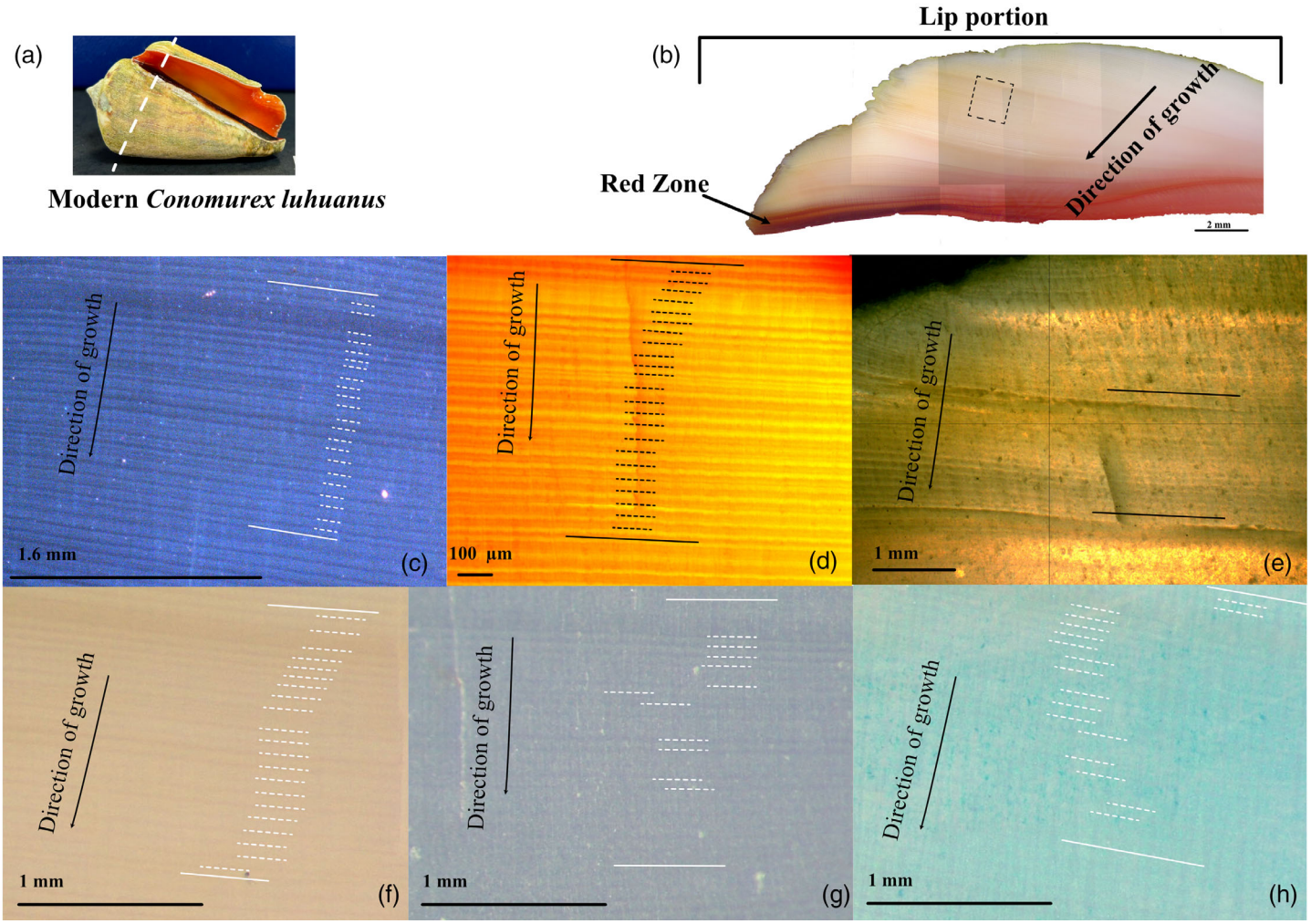

Fig. 1. Images of targeted areas using different methods on modern *C. luhuanus*. (**a**) Modern *C. luhuanus* (ID:SI30-C1-4), white dashed lines indicate where the shell was cut. (**b**) A cross-section of the lip and the targeted area of counting GIs is indicated by a dark dashed rectangle. CL (**c**), TML (**d**), thin-section (20–35 μm) (**e**), RM (**f**), acetate peel (**g**), and Mutvei's solution (**h**). In TML (d), successive growth increments were visualized more effectively, and the image shows less haze and better contrast compared with RM (f), acetate peel (g), or Mutvei's solution (h). Thin-sectioning (e) failed to enhance GI visualization. The area selected for counting and measuring GIs was defined by two solid lines extending from the first to the last counted increment. The short dashed lines show the daily growth lines (GLs), and the area between two GLs is a GI (daily growth increments influenced by lunar-tidal cycles). The absence of short dashed lines within the targeted area suggests that the GLs were not easily detectable. The scale bar is different for each image.

WiRE 5.3 software with an average of 1 s of laser exposure and 3 repetitions to collect data. Spectra between 90 and 1100 cm^{-1} are the wavelengths used to distinguish between calcium carbonate polymorphs. Before analyzing the specimens, a fragment of coral along with synthetic calcite was analyzed as external standards to calibrate and identify key interpretative bands. Baseline correction and smooth methods for acquired spectra were not used, as no extra noise was detected. Our data showed that all samples were aragonite (Supporting Information Fig. S4). To acquire images using CRM, the surface of the shell sections were mapped and multiple scans were conducted.

After non-staining methods, we performed acetate peel replicas and Mutvei's solution in the same section, but for FS93-XU36-9 and C-13, Mutvei's solution was performed on the mirror sections (Table 2). We followed Ropes (1984, 1987) to prepare acetate peel replicas of the shell surface. To do so, we immersed the surface of the cross-section of the shells in 1% HCl for 3 min. After rinsing the samples using deionized water, the slides were left under a fume hood until dried. To create a peel, acetone was flooded onto the surface of the etched cross-section shells, and then an acetate replica was gently unfolded (Cellulose Acetate, thickness 35 μm) (Ropes 1984, 1987). For a successful peel, we left the sample to dry for 24 h then gently removed the acetate peel. The acetate

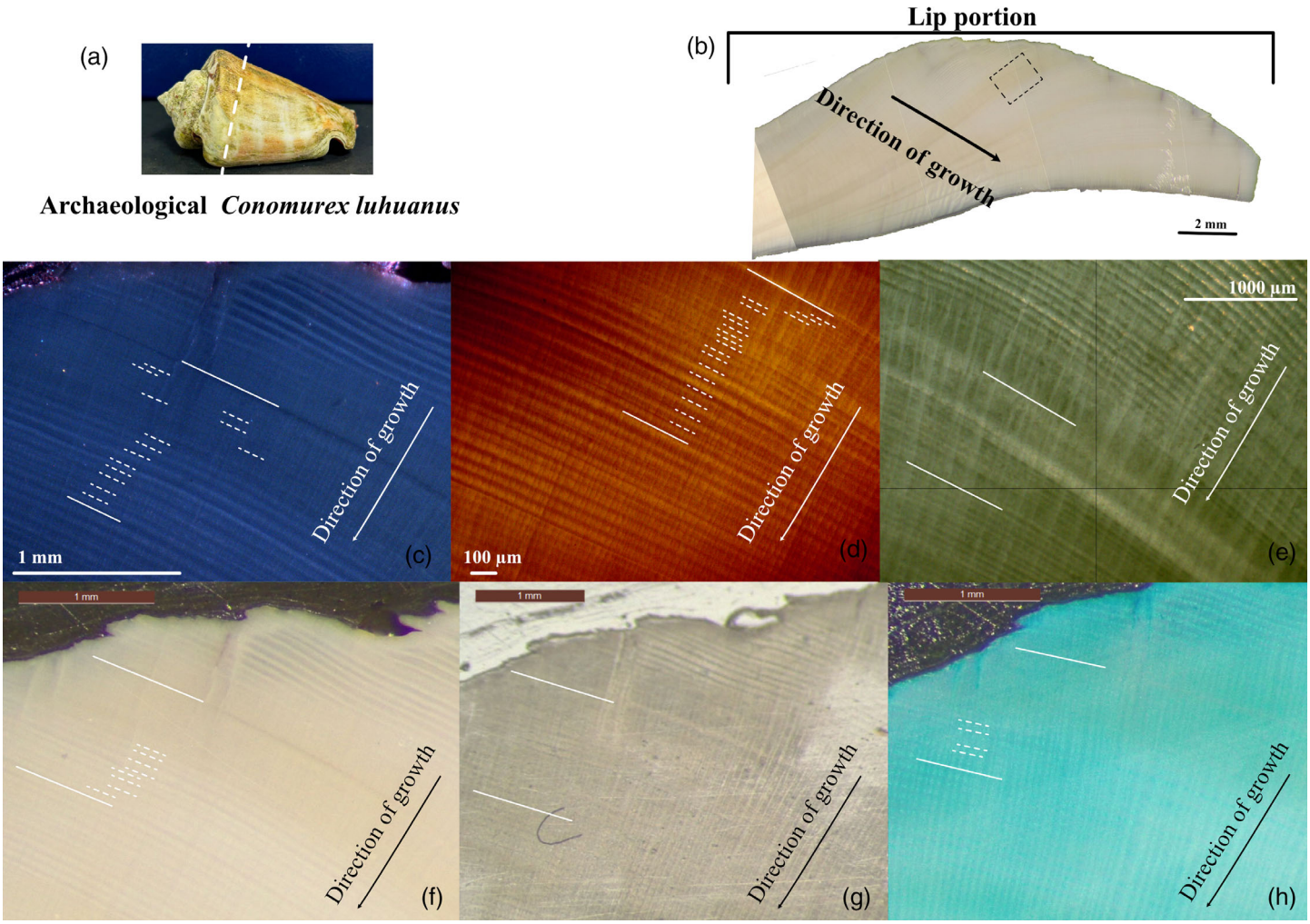

Fig. 2. Images of targeted areas using different methods on archaeological *C. luhuanus*. (**a**) Archaeological *C. luhuanus* (ID No: FS26-XU10-4), white dashed line indicates where the shell was sectioned. (**b**) A cross-section of the lip with the targeted area shown by a dark dashed rectangle. CL (**c**), TML (**d**), thin-section (20–35 μm) (**e**), RM (**f**), acetate peel (**g**), and Mutvei's solution (**h**). In TML (d), successive growth increments were visualized more effectively, and the image showed less haze and better contrast compared with RM (f), and acetate peel (g) or Mutvei's solution (h). Thin-sectioning (e) and acetate peel (g) failed to enhance GI visualization. The area selected for counting and measuring GIs was defined by two solid lines extending from the first to the last counted increment. The short dashed lines show the daily growth lines (GLs), and the area between two GLs is a GI (daily growth increments influenced by lunar-tidal cycles). The absence of short dashed lines within the targeted area suggests that the GLs were not easily detectable. The scale bar is different for each image.

peel replica was observed under a stereomicroscope. For the staining method, we used Mutvei's solution, which contains acetic acid, glutaraldehyde, and alcian blue powder. The timing for immersing samples in this solution is between 5 min to 4 h depending on the shell material and aims of the study (Schöne et al. 2005). We decreased the staining time to 8 min at 37°C, as Schöne et al. (2005) suggested for marine gastropod shells, to minimize the interference of stained crossed-lamellar patterns on visualizing growth increments (GIs). Acetate peel and stained specimens were examined under the reflected stereomicroscope. We adjusted the light balance to obtain the most appropriate depiction of the GIs under a stereomicroscope.

Additionally, to investigate the impact of the thickness of sections on growth increment visibility, we used a thin-section cut-off saw and grinder for preparing thin sections. After each grinding, the thickness of the shell was checked to prevent unintended loss of shell material. This process required approximately 10–15 min for each slide. Afterward, to achieve a smooth surface, manual grinding was performed using 2000, 3000, and 5000 grit paper, and polishing was performed using 1-µm aluminum oxide powder in suspension on a Buehler polishing cloth. We created thin sections (25–30 μm) for two cross-section shells to visualize growth increments (GIs) under TML (Table 2).

Table 2. Eight *Conomurex luhuanus* samples were investigated in this study. N (No) indicates that methods were not applied to a specimen, while Y (Yes) indicates methods were applied, but GIs were not successfully counted in the chosen area. This was because GIs were unclear when using acetate peel and thin section methods, and using CRM was too expensive and time-consuming to analyze every specimen. Furthermore, this sample set was being used for oxygen isotope analysis as part of another ongoing study, so it was not possible to apply all methods uniformly across all shells as some sections were needed for geochemical analysis. (*) indicates that the method was not performed in the same section; instead, the mirror section was used. The relevant images are shown in Figs. 1, 2 and Supporting Information Figs. S2, S3. Modern shells were collected in two different years, 2019 and 2023; and we focus on larger shells (> ~50mm) in this study.

			The number of GIs counted using different methods						
Specimens	Shell ID	Estimated age (yr)	TML	CRM	CL	Thin section	Acetate peel	Mutvei's solution	RM
Modern shells	SI30-C1-4 (2023)	~ 1	24	Y	23	Y	12	18	22
	SI30-C1-9 (2023)	~ 1	13	Y	13	N	N	N	13
	C-13 (2019)	~ 1	19	N	19	N	N	18*	19
	SI30-C1-3 (2023)	~ 1	5	N	Y	N	N	N	5
Archaeological shell	FS26-XU10-4	~ 1	20	Y	15	Y	Y	5	9
	FS93-XU36-9	~1	19	Y	18	N	16	18*	17
	FS93-XU36-11	~ 1	19	N	11	N	N	N	Y
	XU10-14	~ 1	24	N	24	N	N	N	24

Assessment

Conomurex luhuanus, similar to other *Conomurex* spp. and other intertidal mollusk species, shows daily growth increments that are modulated by lunar-tidal cycles (Schöne and Surge 2012; Hausmann et al. 2017; *see* Fig. S2 in Alidoostsalimi et al. 2025). Red coloration was observed at the lip edge of some modern shells, forming a red zone containing very narrow growth increments, which appear as thick or dense red lines, likely resulting from either paused or slowed growth during the cold season (e.g., Figs. 1, 3) (Alidoostsalimi et al. 2025). The red zone is formed by carotenoid pigments, which have been reported by Hausmann et al. (2017). The reason behind its presence is not clear and further studies are required. Similarly, in archaeological samples, we observed brownish thick or dense lines, likely formed during periods of reduced or halted growth in the cold season (Fig. 3d). Nonetheless, the red pigments were not observed, likely due to fading of the pigment over time (Figs. 2, 3). In the red zones of slower growth, we were unable to distinguish GIs using all techniques, as GIs were too narrow (< ~ 20 μm) (Fig. 3). Although we were unable to count the GIs as they were overly narrow in the red zones, we gained an idea of growth patterns in this region using TML (Fig. 3).

In both modern and archaeological samples, microstructural patterns (crossed-lamellar layers) were observed using all techniques (Fig. 3f–k). However, the shell microstructure was clearer under TML and CRM compared with other techniques (Fig. 3). The shell body spiral consists of three different layers (L1–L3), composed of aragonite and showing crossed-lamellar patterns which were visualized by TML, CRM, and Mutvei's solution (Fig. 3f–h). Similar observations are noted in other Stombridae species (e.g., Tojo and Ohno 1999; Radermacher et al. 2009).

In a cross-section, growth lines were generally more distinct from the middle of the lip toward the oldest part of the shell; however, this pattern was not consistent, and in some areas, the growth lines were not clearly visible, making the distinction of GIs difficult. Additional thin growth lines were observed within increments, which may represent sub-increments or microgrowth lines formed in response to tidal currents, short-term environmental, or physiological events. Transmitted-light microscopy was the only method that enabled the observation of these GLs (e.g., sample SI30-C1-9 is shown in Supporting Information Fig. S2).

In the modern sample (SI30-C1-4), each technique revealed a different number of GIs. 22, 23, and 24 GIs were successfully visualized and counted in the targeted region using RM, CL, and TML, respectively. Mutvei's solution (18) and acetate peel (12) revealed a smaller number of GIs (Fig. 1c–h). However, across techniques, the number of paired successive GIs that could be directly compared ranged from 11 to 22, as some paired successive GIs were not distinguishable with Mutvei's solution, RM, and CL (Figs. 1 and 4). We provided paired width measurement data from successive GIs using CL, TML, Mutvei's solution, and RM. Pairwise Pearson correlations suggest that the average absolute correlation coefficient across all pairs is $|r| = 0.48$, showing there is a moderate level of agreement across all techniques. The correlations between TML-Mutvei's solution and CL-Mutvei's solution were $r = 0.68$ and $p < 0.05$. A moderate correlation was observed for TML-CL ($r = 0.44$, $p < 0.05$) and TML-RM ($r = 0.47$, $p > 0.05$). Other pairwise correlations were not significant ($p > 0.05$) due to the small number of paired successive GIs (Fig. 4). Cronbach's α values (0.67) also suggest that there is acceptable consistency across methods. However, the intraclass correlation coefficient

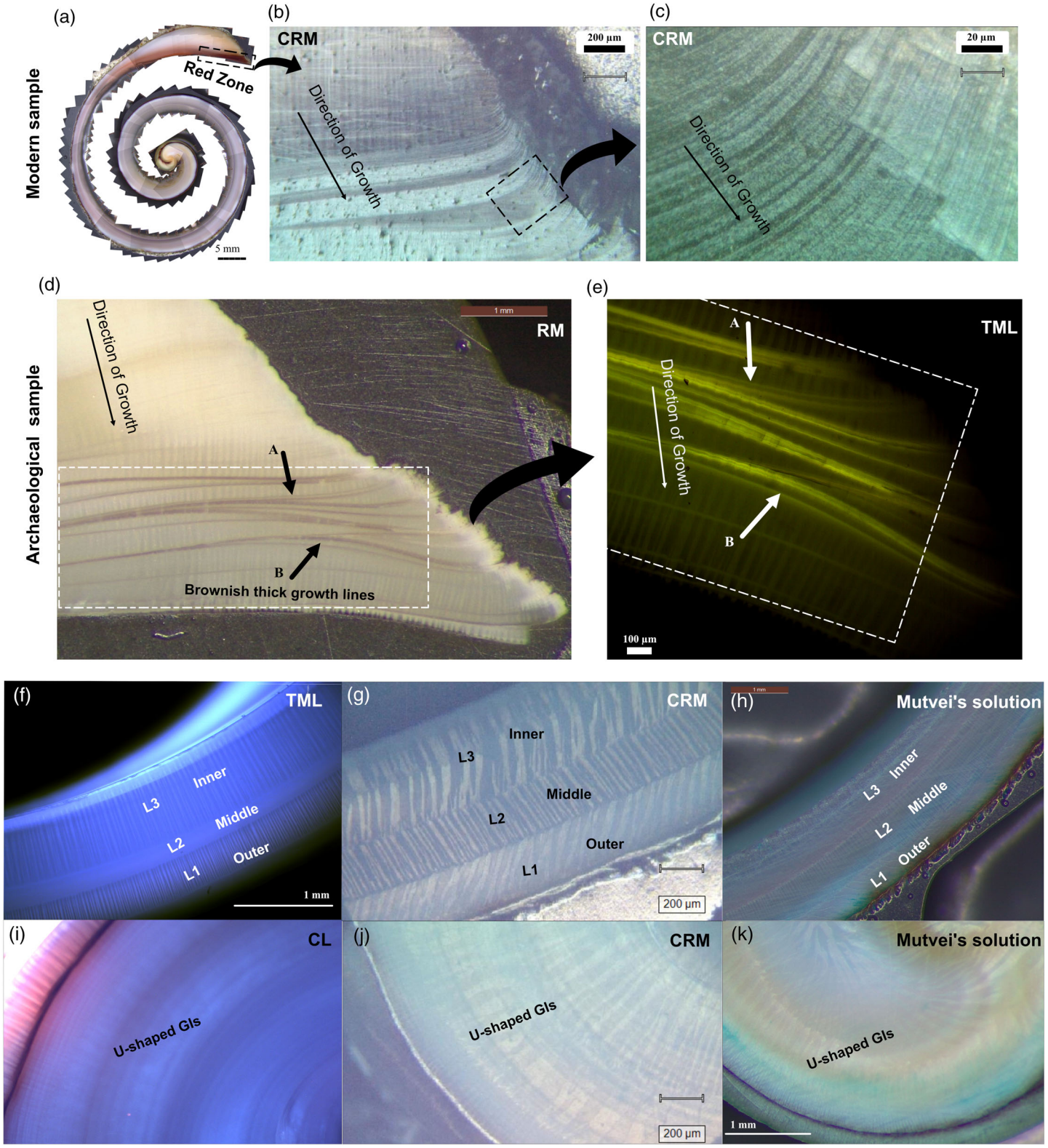

Fig. 3. Legend on next page.

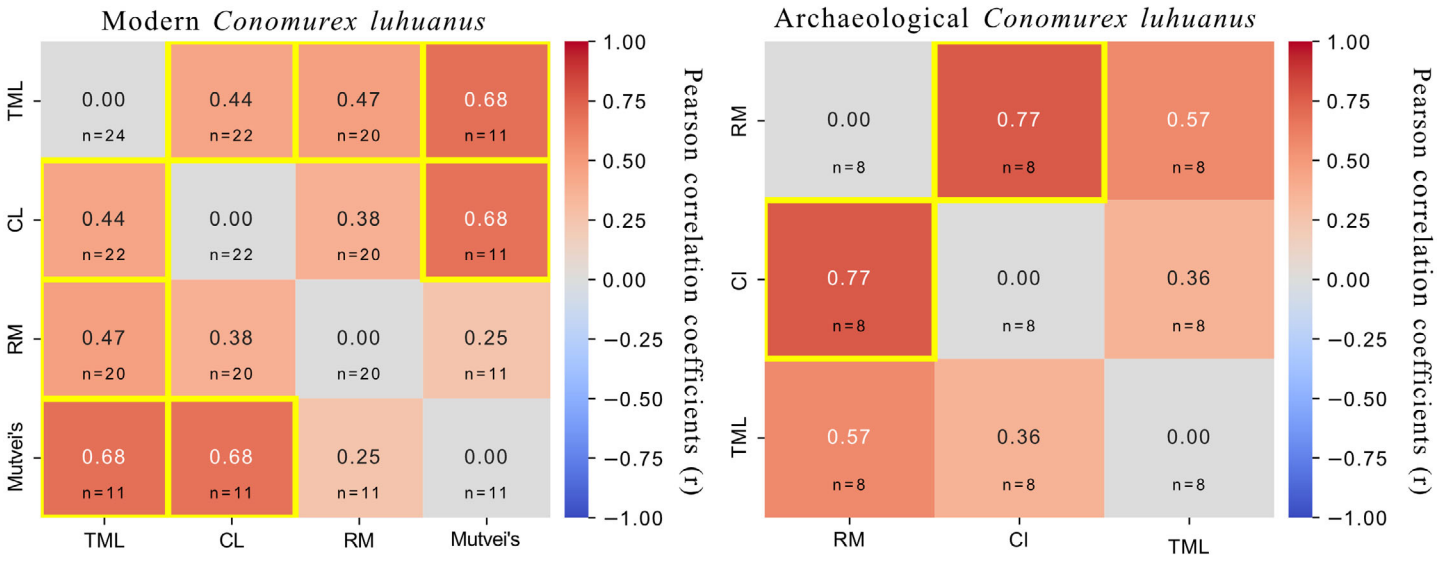

Fig. 4. Correlation heatmap matrices for modern and archaeological shells perfomed using Python software (version 3.8.8) to compare different approaches in measuring successive GIs in the modern (left) and archaeological (right) *C. luhuanus* shells. Thin section and acetate peel did not visualize paired successive GIs in the selected area for both modern and archaeological shells. In archaeological shells, we also did not detect enough paired successive GIs in the determined area using Mutvei's solution for statistically robust comparisons. Therefore, their data was not used for statistical tests. The same GIs were examined, but the number of visible successive GIs varied among methods due to differences in resolution, contrast, and the ability of each method to reveal GIs. Between 11 and 22 paired successive GIs were measured in the modern samples paired using CL, TML, Mutvei's solution, and RM. Eight paired successive GIs were measured for archaeological samples using TML, CL, and RM. The correlation was only performed for data points obtained from the paired successive GIs where results were available from methods. Moderate correlations (e.g., $r = 0.57$ or 0.36) were observed between some methods, but these were not statistically significant due to the small number of paired observations. The yellow rectangles in the correlation plot indicate statistically significant relationships ($p < 0.05$). (https://github.com/MahsaAS86/Correlation_Heatmap_Growth_Increments).

(ICC = 0.10, 95% CI [−0.01, 0.37]) shows that the measurement obtained from each technique is not numerically interchangeable, indicating limited consistency among techniques in measuring growth increments.

In the archaeological sample (FS26-XU10-4) also, each technique revealed a different number of GIs. Transmitted-light microscopy revealed a total of 20 GIs in the targeted region (Fig. 2d). We were unable to distinguish and count GIs using the acetate peel method, so these were not included in the statistical analyses (Fig. 2g). Cathodoluminescence microscopy, RM, and Mutvei's solution revealed 15, 9, and 5 GIs, respectively (Fig. 2c,f,h). As for archaeological samples, paired width measurement data from successive GIs were obtained from CL, TML, and RM ($n = 8$ GIs) (Figs. 2, 4). Pairwise Pearson correlations show the average absolute correlation coefficient was $|r| = 0.57$, suggesting there is a strong correlation across the methods. A strong significant correlation was observed RM-CL ($r = 0.77$, $p < 0.05$). Other pairwise correlations were not significant ($p > 0.05$) due to a small number of paired successive GIs. However, a moderate correlation was observed for RM-TML ($r = 0.57$) and CL-TML ($r = 0.36$) (Fig. 4). Cronbach's alpha was $\alpha = 0.79$, indicating that internal consistency between methods is acceptable (they broadly measure similar features). The intraclass correlation coefficient (ICC(2) = 0.35 [95% CI = −0.01 to 0.76]) suggested low to moderate consistency in absolute values across techniques (inter-method agreement), but the confidence interval was wide due to the small number of samples ($n = 8$).

Overall, these results suggest that although all methods measured the same feature, differences in resolution, scale, and contrast offered by each method can lead to slight differences in absolute width values. Additionally, it is important to

Fig. 3. Narrow growth increments in the red zone appear as thick or dense lines (a-e), and shell microstructure of *C. luhuanus* (f-k). (**a**) modern shell cross-section. The dashed rectangle shows the red zone (detail in **b** and **c**) at the edge of the lip, corresponding to a region of slowed or halted growth. This area with narrow growth increments (< ~ 20 μm) remains uncountable and indistinct, even when using CRM (b and c). (**d**) Very narrow growth increments in an archaeological shell cross-section. The thick brownish lines correspond to a region of slowed or halted growth. This area is similar to the red zone observed in modern samples, but the red pigments are noticeably faded in archaeological samples. (**e**) The thick brownish lines under TML remain uncountable and indistinct. The arrows (a and b) in images d and e highlight corresponding linear features in both images. (**f–h**) The shell body spiral consists of three different layers (L1–L3). (**i–k**) Columella fold with a sequence of thick and thin growth increments (as described by Tojo and Ohno 1999) visualized using CL (i), CRM (j), and Mutvei's solution (k). The crossed-lamellar pattern can be observed in G. Overall, shell structures are clearest using TML and CRM. The arrows and quadrats are approximate rather than exact locations. The scale bar is different for each image.

note that TML revealed more GIs compared with the other techniques, making direct comparison of all GIs impossible. The significant correlation was based on paired successive GIs across all methods, rather than on the total counted GIs.

In both modern and archaeological samples, thin sections (25–30 μm) not only failed to enhance the visibility of growth increments but also made GIs hazier, especially for the narrow GIs (< 30 μm). Likewise, distinguishing GIs using acetate peel was also challenging (Figs. 1e, 2e). For CRM, mapping the whole targeted region at 50× magnification was time-consuming, and changing the magnification was not feasible as the GIs became indiscernible at low magnification. Consequently, it was impractical and unfeasible to measure and count the GIs for both modern and archaeological samples using CRM.

Discussion

Overall, our results suggested that if GIs in the selected area were clear under RM, this clarity was maintained across other techniques; and in the absence of slowed or halted growth, there is a broadly consistent correlation ($r = 0.4$ to 0.7, $p < 0.05$) using Mutvei's solution, TML, and CL (Fig. 4). This suggests that all methods can be considered as an appropriate alternative to Mutvei's solution when the GIs are easy to distinguish. Likewise, previous studies on long-lived bivalves (e.g., *A. islandica*) showed that Raman spectroscopy and fluorescence microscopy can provide results comparable to Mutvei's solution for visualizing growth increments with the advantage of requiring only minimal physical sample preparation and no chemical pretreatment (Wanamaker et al. 2009; Beierlein et al. 2015). Nonetheless, a gap in previous research is the investigation of how alternative techniques can visualize GIs when they are not easily visible using Mutvei's solution. This is particularly evident in cases where growth lines are thin, so it was not easy to distinguish GIs. Notably, in our samples (both modern and archaeological), TML was the only method that enabled the GIs to be visualized, particularly in the region where other approaches (specifically, Mutvei's solution) were unsuccessful in distinguishing growth increments because the GLs were thin (Figs. 1, 2; Supporting Information Figs. S2, S3).

Our research shows that TML on thick sections (2–3 mm) is an alternative option for visualizing daily and sub-daily GIs in short-lived marine gastropods. Likewise, other researchers have shown that TML can characterize sub-annual to daily growth increments in other mollusk shells (Welsh et al. 2011; Wang et al. 2012; Mills et al. 2023). The success of visualizing GIs using TML is likely due to the light passing through the cross-sectioned shells toward the objective lens, which might aid in enhancing contrast. For example, Wang et al. (2012) suggested that TML enhanced the visibility of winter growth bands in limpets (Wang et al. 2012). Other than daily growth increments, we could discern growing periods as darker shadow/lines corresponding to either growth declines or cessations followed by light shadow/bands corresponding to fast-growing (e.g., Figs. 1d and SI30-C1-9 in S2). Wanamaker et al. (2009) revealed a similar level of information for annual GIs in a long-lived bivalve using fluorescence spectroscopy. They inferred darker lines contain less (fluorescence) organic material in the aragonite shells corresponding to a slow growth/growth session (Wanamaker et al. 2009). Our observations align with this inference, as dark growth shadow/bands likely formed during low tide and/or at the beginning of rising tide when shells absorb less organic material due to growth slowing or cessation (Schöne 2008; Schöne and Surge 2012). Nonetheless, further study is required to interpret this observation.

However, some researchers have criticized TML as a method for examining growth increments due to its inability to discern sub-annual resolution and/or daily growth increments, and the time-consuming nature of thin section preparation (Risk and Pearce 1992; Schöne et al. 2005). This discrepancy might be because prior research combined TML with thin sectioning, since thinning might facilitate light transmission (Schöne et al. 2005). For example, von Leesen (2014) reported foggy and noisy GIs in a thin-sectioned long-lived bivalve using TML. In our study, this combination also failed to reveal GIs in both modern and archaeological samples. We did not find an explanation in sclerochronology research to interpret this failure, but one explanation for this discrepancy might be the size of the increments under examination. In rock specimens, researchers have observed that when the size of individual particles of interest "… is less than the thickness of the thin section, the particle boundaries tend to become obscured by the overlap of the particles," with smaller particles being more difficult to observe, particularly when there is little difference in the optical properties of adjacent particles (e.g., refraction, color, and birefringence) (Federal Highway Administration 2006). This would certainly also be the case with thin biogenic carbonate growth increments. In our samples, the width of GIs varied across the lips. We still observed thicker GIs (~ 50 μm) in thin sections under TML, but narrow GIs (< 25–30 μm) which were related to slow growth parts were ambiguous and unclear (Figs. 1e, 2e), inhibiting counting. Additionally, we lose shell material after making thin sections, making it challenging to locate visual features of the GIs and compare identical GIs. We also tested 1 mm thick sections, but the results were not significantly different compared with 2–3 mm thick sections commonly used in sclerochronology. Therefore, we suggest that previous concerns about the effectiveness of TML in sclerochronology might be related to using unsuitably thin sections (less than 1 mm) to observe GIs under TML, leading to the acquisition of more noisy images.

Confocal Raman Microspectroscopy enables rapid survey of samples, guiding, and supplementing Raman analyses. However, mapping a large area at high resolution to provide an

image is time-consuming and, therefore, expensive as it was mentioned by Beierlein et al. 2015. This issue prevented us from counting all GIs in the targeted area for both modern and archaeological samples using CRM. Cathodoluminescence microscopy is one of the most common analytical tools in Geography and Earth Science departments to study minerals and rocks. Few studies, however, have applied the technique to sclerochronology (Pagel et al. 2000; Barbin 2013; Mouchi et al. 2020). Under CL, the GIs in the aragonite shell showed dull dark bluish to light blue luminescing bands due to insufficient Mn^{2+} in their shells to generate cathodoluminescence (Figs. 1c, 2c) (Barbin 2013; Pagel et al. 2000). In this study, changes in the luminescence color were not detected in the cross-sections of modern and archaeological specimens, showing that the daily growth patterns were not affected by different mineralogy (Barbin 2013; Pagel et al. 2000). Additionally, our Raman data show that diagenesis did not occur in archaeological samples, and samples were well-preserved (Supporting Information Fig. S4). Barbin (2013) suggested that CL can reveal growth increments (including daily increments) that are not visible using TML. Nonetheless, in our study, CL did not enhance increment visualization as much as TML. This could be attributed to the fact that for CL to successfully image biogenic carbonates, such as shells, there must be sufficient Mn^{2+} in the structures. In mollusks, the uptake of Mn^{2+} is linked with physio-chemical variations in the surrounding environment, metabolic activity, and the phylogeny of each species; therefore, not all species are good candidates for CL (Barbin 2013). This research highlights the importance of comparing multiple methods rather than adhering to established techniques, as different methods can enhance GI visualization in certain samples over others. We suggest prioritizing TML (with thick sections) as an alternative option in sclerochronology, particularly where established methods are unable to distinguish narrow GIs. Transmitted-light microscopy enables sclerochronologists to obtain more detailed information about shell growth patterns. As TML is particularly effective in distinguishing narrow growth increments where other methods have failed, this method may facilitate new insights in sclerochronological studies of day length, tidal currents, and ultradian growth lines (e.g., Berry and Barker 1968; Schöne 2008).

Comment and recommendations

Leonardo da Vinci stated, "We could not count, in the shells of cockles and snails, the years and months of their life …" (quoted in Jones 1983). Sclerochronology, however, enables researchers to do just this—study growth increments in biological carbonates (e.g., marine gastropods). In this study, we conducted the first comparative research on visualizing GIs in intertidal short-lived marine gastropods, comparing different techniques against Mutvei's solution for *C. luhuanus*. Each method has distinct advantages and disadvantages, which should be considered when choosing the approach to investigate GIs. We conclude the following (*see* Table 3).

- TML is a simple, quick, non-destructive, and cost-effective technique when used on thick sections (2–3 mm). TML can distinguish narrow GIs where other methods fail. It also has the potential to provide detailed information about subdaily growth patterns. It could offer new insights into sclerochronological studies of day length and tidal current. Such detailed information is also valuable for ecological physiology, as it highlights how shell growth rates change in response to changing conditions. Additionally, as no chemical treatment or stain is applied, the section can be directly used for geochemical and archaeological analysis. Moreover, for this method, providing a well-polished surface is not necessary.
- In TML, the quality of images has less interference from the shell crystal structure than in other methods such as Mutvei's solution, so it may be a better method to investigate GIs in shells with crossed-lamellar patterns (e.g., short-lived marine gastropods).
- A thin section is not required for investigating GIs under TML, as it was suggested previously. However, different shells might have different levels of transparency due to the carbonate density. For our samples, we obtained maximum illumination using a common sclerochronology thickness, 2–3 mm. Before staining (Mutvei's solution) or using other destructive and/or expensive techniques, we highly recommend trying TML, particularly for observing parts of the shells where growth bands are foggy and noisy under RM, and Mutvei's solution cannot distinguish GIs.
- The efficacy of both Mutvei's solution and CL in sclerochronology is related to the chemical and structural characteristics of the shells. For CL, shells must contain sufficient Mn^{2+} to be effective, which is not the case for all species. For Mutvei's solution, the effectiveness of the stain in enhancing growth increments is species-dependent, relating to the shell crystal structure and amount of polysaccharides in the shell. Both of these methods may not provide the level of detailed information that TML can provide.
- Confocal Raman Microspectroscopy is a common, powerful, and non-destructive technique that is well established in sclerochronology for determining the shell calcium carbonate polymorph. Although CRM has the potential to visualize fine growth bands in marine gastropod shells ($< \sim 20\ \mu m$), mapping a larger area of the shell is time-consuming and expensive.

Future work recommendation

- Further study is required to understand how sample preservation, in particular for archaeological samples, affects the visibility of growth increments using different methods
- To investigate the effectiveness of TML in visualizing successive GIs using thick sections, more studies using different short- and long-lived species are required.

Table 3. The advantages and disadvantages of the applied methods in visualizing GIs in this study.

Methods	Advantages	Disadvantages
TML	• Non-destructive • Visualize narrow growth lines • Visualize shell microstructure • Grinding and polishing are not necessary • Suitable for shells with crossed-lamellar patterns • Provide detailed lunar daily information (e.g., tides) • Visualize daily (or sub-daily) growth increments • Section can subsequently be used for geochemical analysis • A thin section is not necessary	• Need to adjust light sources to enhance the contrast • Success depends on carbonate density
CL	• Non-destructive • Visualize daily growth increments • Visualize shell microstructure • Determine the shell mineralogy • Section can subsequently be used for geochemical analysis	• Unable to visualize sub-daily growth increments • Success depends on the chemical properties (Mn^{2+}) of shells (species specific)
CRM	• Non-destructive • Visualize narrow growth increments • Visualize shell microstructure • Determine the crystal structure and carbonate polymorph • Section can subsequently be used for geochemical analysis	• Mapping a large area of the shells is time-consuming and expensive
Mutvei's solution	• Visualize daily increments • Works for a wide range of biogenic archives • Widely used in sclerochronology studies	• Requires additional sample preparation • Slightly destructive and toxic (requires chemicals) • Success depends on shell characteristics • Challenging for shells with crossed-lamellar patterns • Section cannot subsequently be used for geochemical analysis (requires paired cross-section for geochemical analysis)
Acetate peel	• Visualize daily increments • Works for long-lived shells (*Arctica*)	• Requires additional sample preparation • Slightly destructive (requires chemicals) • Introduces noise to the growth records • Unable to adequately replicate the physical feature of the GIs • Challenging for shells with crossed-lamellar patterns

- Conducting controlled tank growth experiments or field-based mark-recapture studies may aid in understanding the time period represented in incremental growth structures and investigate the effectiveness of each technique in visualizing GIs.

Author Contributions

Mahsa Alidoostsalimi and Amy L. Prendergast conceived the study. Mahsa Alidoostsalimi co-led the manuscript development under Amy L. Prendergast's supervision. Mahsa Alidoostsalimi conducted experiments, analyzed the data, and wrote the original draft. Amy L. Prendergast contributed to writing (review and edit). Russell N. Drysdale, Ian J. McNiven, Ariana B. J. Lambrides, and Sean Ulm contributed to reviewing and editing the manuscript. Mahsa Alidoostsalimi, Amy L. Prendergast, Ian J. McNiven, Ariana B. J. Lambrides, and Sean Ulm conducted the field survey. Nguurruumungu Indigenous Corporation and Walmbaar Aboriginal Corporation RNTBC provided permission to work on samples. Mahsa Alidoostsalimi used Generative Artificial intelligence tools (AI) to correct grammatical errors and improve the clarity in a few sentences.

Acknowledgments

We acknowledge Dingaal and Ngurrumungu Traditional Owners as partners in this research. This work was largely undertaken on the unceeded lands of the Wurundjeri People in Naarm, Melbourne. We pay our respects to their elders past and present. This work was performed in part at the Materials Characterization and Fabrication Platform (MCFP) and the

Victorian Node of the Australian National Fabrication Facility (ANFF) and in part at the Trace Analysis for Chemical, Earth, and Environmental Sciences (TraACEES) Platform at the University of Melbourne. We acknowledge Anders Barlow and Ling Chung for their support with the description of services. Additionally, we acknowledge Malcolm Wallace and Ashleigh Hood from the School of Geography, Earth, and Atmospheric Science at the University of Melbourne for their support in using facilities (Cathodoluminescence and a thin section cut-off saw and grinder) in their laboratory. This research was supported by the Australian Research Council Centre of Excellence of Australian Biodiversity and Heritage (project number CE170100015) and the Australian Research Council Centre of Excellence for Indigenous and Environmental Histories and Futures (project number CE230100009). Amy L. Prendergast was supported by an Australian Research Council DECRA Fellowship during the course of this research (DE200100890). Open access publishing facilitated by The University of Melbourne, as part of the Wiley - The University of Melbourne agreement via the Council of Australian University Librarians.

Conflicts of Interest

All data are initially presented in this journal. We declare that there is no conflict of interest regarding the publication of this paper. Archaeological fieldwork on Lizard Island was conducted under Queensland Government Department of Environment and Heritage Protection Permits WITK17615716 and PTU18-001110. Live-collected shell and seawater samples were collected under Marine Parks Permit G23/47045.1. This study did not involve endangered or protected species.

Data Availability Statement

All data have been included in the appendices (Supporting Information).

References

Alidoostsalimi, M., A. L. Prendergast, S. Ulm, et al. 2025. "Sclerochronology and Oxygen Isotope Variations in Modern *Conomurex luhuanus* Shells: An Archive for Reconstructing Palaeotemperature and Shellfish Gathering on the Great Barrier Reef, Australia." *Palaeogeography, Palaeoclimatology, Palaeoecology* 659: 112633. https://doi.org/10.1016/j.palaeo.2024.112633.

Álvarez, M., I. B. Godino, A. Balbo, and M. Madella. 2011. "Shell Middens as Archives of Past Environments, Human Dispersal and Specialized Resource Management." *Quaternary International* 239, no. 1/2: 1–7. https://doi.org/10.1016/j.quaint.2010.10.025.

Andrus, C. F. T. 2011. "Shell Midden Sclerochronology." *Quaternary Science Reviews* 30, no. 21/22: 2892–2905. https://doi.org/10.1016/j.quascirev.2011.07.016.

Barbin, V. 2013. "Application of Cathodoluminescence Microscopy to Recent and Past Biological Materials: A Decade of Progress." *Mineralogy and Petrology* 107: 353–362. https://doi.org/10.1007/s00710-013-0266-6.

Beierlein, L., G. Nehrke, and T. Brey. 2015. "Confocal Raman Microscopy in Sclerochronology: A Powerful Tool to Visualize Environmental Information in Recent and Fossil Biogenic Archives." *Geochemistry, Geophysics, Geosystems* 16, no. 1: 325–335. https://doi.org/10.1002/2014GC005547.

Berry, W. B., and R. M. Barker. 1968. "Fossil Bivalve Shells Indicate Longer Month and Year in Cretaceous Than Present." *Nature* 217, no. 5132: 938–939. https://doi.org/10.1038/217938b0.

Burchell, M., N. Hallmann, A. Martindale, A. Cannon, and B. R. Schöne. 2013. "Seasonality and Intensity of Shellfish Harvesting on the North Coast of British Columbia." *Journal of Island and Coastal Archaeology* 8, no. 2: 152–169. https://doi.org/10.1080/15564894.2013.787566.

Burchell, M., M. P. Stopp, A. Cannon, N. Hallmann, and B. R. Schöne. 2018. "Determining Seasonality of Mussel Collection From an Early Historic Inuit Site, Labrador, Canada: Comparing Thin-Sections With High-Resolution Stable Oxygen Isotope Analysis." *Journal of Archaeological Science: Reports* 21: 1215–1224. https://doi.org/10.1016/j.jasrep.2018.02.016.

Butler, P. G., and B. R. Schöne. 2017. "New Research in the Methods and Applications of Sclerochronology." *Palaeogeography, Palaeoclimatology, Palaeoecology* 465: 295–299. https://doi.org/10.1016/j.palaeo.2016.11.013.

Carré, M., I. Bentaleb, M. Fontugne, and D. Lavallee. 2005. "Strong El Niño Events During the Early Holocene: Stable Isotope Evidence From Peruvian Sea Shells." *The Holocene* 15, no. 1: 42–47. https://doi.org/10.1191/0959683605h1782rp.

Carré, M., J. P. Sachs, A. J. Schauer, W. E. Rodríguez, and F. C. Ramos. 2013. "Reconstructing El Niño-Southern Oscillation Activity and Ocean Temperature Seasonality From Short-Lived Marine Mollusk Shells From Peru." *Palaeogeography, Palaeoclimatology, Palaeoecology* 371: 45–53. https://doi.org/10.1016/j.palaeo.2012.12.014.

Catterall, C. P., and I. R. Poiner. 1983. "Age- and Sex-Dependent Patterns of Aggregation in the Tropical Gastropod *Strombus luhuanus*." *Marine Biology* 77: 171–182. https://doi.org/10.1007/BF00396315.

Colonese, A. C., M. A. Mannino, D. B. Y. Mayer, et al. 2011. "Marine Mollusc Exploitation in Mediterranean Prehistory: An Overview." *Quaternary International* 239, no. 1/2: 86–103. https://doi.org/10.1016/j.quaint.2010.09.001.

Cornu, S., J. Pätzold, E. Bard, J. Meco, and J. Cuerda-Barcelo. 1993. "Paleotemperature of the Last Interglacial Period Based on $\delta_{18}O$ of *Strombus bubonius* From the Western Mediterranean Sea." *Palaeogeography, Palaeoclimatology, Palaeoecology* 103, no. 1/2: 1–20. https://doi.org/10.1016/0031-0182(93)90047-M.

Ekaratne, S. U. K., and D. J. Crisp. 1982. "Tidal Micro-Growth Bands in Intertidal Gastropod Shells, With an Evaluation of Band-Dating Techniques." *Proceedings of the Royal Society of London, Series B: Biological Sciences* 214, no. 1196: 305–323. https://doi.org/10.1098/rspb.1982.0013.

Etayo-Cadavid, M. F., C. F. T. Andrus, K. B. Jones, et al. 2013. "Marine Radiocarbon Reservoir Age Variation in *Donax obesulus* Shells From Northern Peru: Late Holocene Evidence for Extended El Niño." *Geology* 41, no. 5: 599–602. https://doi.org/10.1130/G34065.1.

Faulkner, P., A. Thangavelu, R. Ferguson, et al. 2020. "Middle to Late Holocene Near-Shore Foraging Strategies at Caution Bay, Papua New Guinea." *Journal of Archaeological Science: Reports* 34: 102629. https://doi.org/10.1016/j.jasrep.2020.102629.

Federal Highway Administration Research and Technology. 2006. "*Petrographic Methods of Examining Hardened Concrete: A Petrographic Manual*." Chapter 5: Preparation of Specimens for Optical Microscopy. Publication Number: FHWA-HRT-04150. https://www.fhwa.dot.gov/publications/research/infrastructure/pavements/pccp/04150/chapt5.cf.

Fenger, T., D. Surge, B. Schöne, and N. Milner. 2007. "Sclerochronology and Geochemical Variation in Limpet Shells (*Patella vulgata*): A New Archive to Reconstruct Coastal Sea Surface Temperature." *Geochemistry, Geophysics, Geosystems* 8, no. 7. https://doi.org/10.1029/2006GC001488.

García-Escárzaga, A., I. Gutiérrez-Zugasti, M. R. González-Morales, A. Arrizabalaga, J. Zech, and P. Roberts. 2020. "Shell Sclerochronology and Stable Oxygen Isotope Ratios From the Limpet *Patella depressa* Pennant, 1777: Implications for Palaeoclimate Reconstruction and Archaeology in Northern Spain." *Palaeogeography, Palaeoclimatology, Palaeoecology* 560: 110023. https://doi.org/10.1016/j.palaeo.2020.110023.

Giovas, C. M. 2016. "Though She Be But Little: Resource Resilience, Amerindian Foraging, and Long-Term Adaptive Strategies in the Grenadines, West Indies." *Journal of Island and Coastal Archaeology* 11, no. 2: 238–263. https://doi.org/10.1080/15564894.2016.1193572.

Gosling, E. 2008. Bivalve Molluscs: Biology, Ecology and Culture. John Wiley & Sons.

Gutiérrez-Zugasti, I., A. García-Escárzaga, J. Martín-Chivelet, and M. R. González-Morales. 2015. "Determination of Sea Surface Temperatures Using Oxygen Isotope Ratios From *Phorcus lineatus* (Da Costa, 1778) in Northern Spain: Implications for Paleoclimate and Archaeological Studies." *Holocene* 25, no. 6: 1002–1014. https://doi.org/10.1177/0959683615574892.

Gutiérrez-Zugasti, I., R. Suárez-Revilla, A. García-Escárzaga, et al. 2025. "Shell Sclerochronology of the Limpet Patella Ferruginea Gmelin, 1791: Implications for Growth Patterns and Reconstruction of Past Sea Surface Temperatures." *Palaeogeography, Palaeoclimatology, Palaeoecology* 670: 112954. https://doi.org/10.1016/j.palaeo.2025.112954.

Guzman, N., A. D. Ball, J. P. Cuif, Y. Dauphin, A. Denis, and L. Ortlieb. 2007. "Subdaily Growth Patterns and Organo-Mineral Nanostructure of the Growth Layers in the Calcitic Prisms of the Shell of *Concholepas concholepas* Bruguière, 1789 (Gastropoda, Muricidae)." *Microscopy and Microanalysis* 13, no. 5: 397–403. https://doi.org/10.1017/S1431927607070705.

Hausmann, N., A. C. Colonese, A. de Lima Ponzoni, et al. 2017. "Isotopic Composition of *Conomurex fasciatus* Shells as an Environmental Proxy for the Red Sea." *Quaternary International* 427: 115–127. https://doi.org/10.1016/j.quaint.2015.08.051.

Hollyman, P. R., V. V. Laptikhovsky, and C. A. Richardson. 2018. "Techniques for Estimating the Age and Growth of Molluscs: Gastropoda." *Journal of Shellfish Research* 37, no. 4: 773–782. https://doi.org/10.2983/035.037.0408.

Hollyman, P. R., M. J. Leng, S. R. Chenery, H. J. Sloane, and C. A. Richardson. 2020. "Calibration of Shell $\delta_{18}O$ From the Common Whelk *Buccinum undatum* Highlights Potential for Palaeoenvironmental Reconstruction." *Palaeogeography, Palaeoclimatology, Palaeoecology* 560: 109995. https://doi.org/10.1016/j.palaeo.2020.109995

Jones, D. S. 1983. "Sclerochronology: Reading the Record of the Molluscan Shell: Annual Growth Increments in the Shells of Bivalve Molluscs Record Marine Climatic Changes and Reveal Surprising Longevity." *American Scientist* 71, no. 4: 384–391. https://www.jstor.org/stable/27852138.

Karney, G. B., P. G. Butler, J. D. Scourse, et al. 2011. "Identification of Growth Increments in the Shell of the Bivalve Mollusc *Arctica islandica* Using Backscattered Electron Imaging." *Journal of Microscopy* 241, no. 1: 29–36. https://doi.org/10.1111/j.1365-2818.2010.03403.x.

Lambrides, A. B., I. J. McNiven, S. J. Aird, et al. 2020. "Changing Use of Lizard Island Over the Past 4000 Years and Implications for Understanding Indigenous Offshore Island Use on the Great Barrier Reef." *Queensland Archaeological Research* 23: 43–109. https://doi.org/10.25120/qar.23.2020.3778.

Liu, C., L. Zhao, N. Zhao, et al. 2022. "Novel Methods of Resolving Daily Growth Patterns in Giant Clam (*Tridacna* Spp.) Shells." *Ecological Indicators* 134: 108480. https://doi.org/10.1016/j.ecolind.2021.108480.

Mannino, M. A., K. D. Thomas, M. J. Leng, and H. J. Sloane. 2008. "Shell Growth and Oxygen Isotopes in the Topshell *Osilinus turbinatus*: Resolving Past Inshore Sea Surface Temperatures." *Geo-Marine Letters* 28: 309–325. https://doi.org/10.1007/s00367-008-0107-5.

Mills, K., E. H. John, D. D. Muir, et al. 2023. "Growth Responses of Mixotrophic Giant Clams on Nearshore Turbid Coral Reefs." *Coral Reefs* 42, no. 2: 593–608. https://doi.org/10.1007/s00338-023-02366-8.

Mouchi, V., L. Emmanuel, V. Forest, and A. Rivalan. 2020. "Geochemistry of Bivalve Shells as Indicator of Shore Position of the 2nd Century BC." *Open Quaternary* 6, no. 1: 4. https://doi.org/10.5334/oq.65.

Nishida, K., M. Peharda, B. R. Schöne, C. Trueman, and M. T. Chung. 2026. "Expanding the Horizons of Sclerochronology: New Perspectives for Life History and Environmental Monitoring." *Limnology and Oceanography Letters* 11, no. 1.

Oschmann, W. 2009. "Sclerochronology." *International Journal of Earth Sciences* 98: 1–2. https://doi.org/10.1007/s00531-008-0403-3.

Pagel, M., V. Barbin, P. Blanc, and D. Ohnenstetter. 2000. Cathodoluminescence in Geosciences: An Introduction, 1–21. Springer Berlin Heidelberg.

Patterson, W. P., K. A. Dietrich, C. Holmden, and J. T. Andrews. 2010. "Two Millennia of North Atlantic Seasonality and Implications for Norse Colonies." *Proceedings of the National Academy of Sciences of the United States of America* 107, no. 12: 5306–5310. https://doi.org/10.1073/pnas.0902522107.

Prendergast, A. L., and B. R. Schöne. 2017. "Oxygen Isotopes From Limpet Shells: Implications for Palaeothermometry and Seasonal Shellfish Foraging Studies in the Mediterranean." *Palaeogeography, Palaeoclimatology, Palaeoecology* 484: 33–47. https://doi.org/10.1016/j.palaeo.2017.03.007.

Prendergast, A. L., R. E. Stevens, T. C. O'Connell, et al. 2016. "Changing Patterns of Eastern Mediterranean Shellfish Exploitation in the Late Glacial and Early Holocene: Oxygen Isotope Evidence From Gastropod in Epipaleolithic to Neolithic Human Occupation Layers at the Haua Fteah Cave, Libya." *Quaternary International* 407: 80–93. https://doi.org/10.1016/j.quaint.2015.09.035.

Radermacher, P., B. R. Schöne, E. Gischler, W. Oschmann, J. Thébault, and J. Fiebig. 2009. "Sclerochronology—A Highly Versatile Tool for Mariculture and Reconstruction of Life History Traits of the Queen Conch, *Strombus GIGAS* (Gastropoda)." *Aquatic Living Resources* 22, no. 3: 307–318. https://doi.org/10.1051/alr/2009043.

Rick, T. C. 2023. "Shell Midden Archaeology: Current Trends and Future Directions." *Journal of Archaeologicl Research* 32, no. 3: 1–58. https://doi.org/10.1007/s10814-023-09189-9.

Risk, M. J., and T. H. Pearce. 1992. "Interference Imaging of Daily Growth Bands in Massive Corals." *Nature* 358, no. 6387: 572–573. https://doi.org/10.1038/358572a0.

Ropes, J. W. 1984. "Procedures for Preparing Acetate Peels and Evidence Validating the Annual Periodicity of Growth Lines Formed in the Shells of Ocean Quahogs, *Arctica islandica*." *Marine Fisheries Review* 46, no. 2: 27–35.

Ropes, J. W. 1987. Preparation of Acetate Peels of Valves From the Ocean Quahog, Arctica islandica, for Age Determinations. Vol. 50. US Department of Commerce, National Oceanic and Atmospheric Administration, National Marine Fisheries Service.

Schöne, B. R. 2008. "The Curse of Physiology—Challenges and Opportunities in the Interpretation of Geochemical Data From Mollusk Shells." *Geo-Marine Letters* 28: 269–285. https://doi.org/10.1007/s00367-008-0114-6.

Schöne, B. R., E. Dunca, J. Fiebig, and M. Pfeiffer. 2005. "Mutvei's Solution: An Ideal Agent for Resolving Microgrowth Structures of Biogenic Carbonates." *Palaeogeography, Palaeoclimatology, Palaeoecology* 228, no. 1/2: 149–166. https://doi.org/10.1016/j.palaeo.2005.03.054.

Schöne, B. R., D. H. Goodwin, K. W. Flessa, D. L. Dettman, and P. D. Roopnarine. 2002. "Sclerochronology and Growth of the Bivalve Mollusks *Chione* (*Chionista*) *fluctifraga* and *C.* (*Chionista*) *cortezi*." *Veliger* 45, no. 1: 45–54.

Schöne, B. R., D. L. Rodland, A. Wehrmann, et al. 2007. "Combined Sclerochronologic and Oxygen Isotope Analysis of Gastropod Shells (*Gibbula cineraria*, North Sea): Life-History Traits and Utility as a High-Resolution Environmental Archive for Kelp Forests." *Marine Biology* 150: 1237–1252. https://doi.org/10.1007/s00227-006-0435-9.

Schöne, B. R., K. Schmitt, and M. Maus. 2017. "Effects of Sample Pretreatment and External Contamination on Bivalve Shell and Carrara Marble $\delta_{18}O$ and $\delta_{13}C$ Signatures." *Palaeogeography, Palaeoclimatology, Palaeoecology* 484: 22–32. https://doi.org/10.1016/j.palaeo.2016.10.026.

Schöne, B. R., and D. M. Surge. 2012. "Part N, Revised, Volume 1, Chapter 14: Bivalve Sclerochronology and Geochemistry." *Treatise Online* 46: 1–24.

Sigma-Aldrich. 2023. "*Sodium acetate, trihydrate (G5882) [Safety data sheet]*." https://doi.org/10.12688/f1000research.129219.2. https://www.sigmaaldrich.com/AU/en/sds/sial/g5882.

Surge, D., and J. H. Barrett. 2012. "Marine Climatic Seasonality during Medieval Times (10th to 12th Centuries) Based on Isotopic Records in Viking Age Shells from Orkney, Scotland." *Palaeogeography, Palaeoclimatology, Palaeoecology* 350: 236–246.

Takamiya, H. 2006. "An Unusual Case? Hunter–Gatherer Adaptations to an Island Environment: A Case Study From Okinawa, Japan." *Journal of Island & Coastal Archaeology* 1, no. 1: 49–66. https://doi.org/10.1080/15564890600585855.

Tojo, B., and T. Ohno. 1999. "Continuous Growth-Line Sequences in Gastropod Shells." *Palaeogeography, Palaeoclimatology, Palaeoecology* 145, no. 1/3: 183–191. https://doi.org/10.1016/S0031-0182(98)00098-4.

Twaddle, R. W., S. Ulm, J. Hinton, C. M. Wurster, and M. I. Bird. 2016. "Sclerochronological Analysis of Archaeological Mollusc Assemblages: Methods, Applications and Future Prospects." *Archaeological and Anthropological Sciences* 8, no. 2: 359–379. https://doi.org/10.1007/s12520-015-0228-5.

Twaddle, R. W., C. M. Wurster, M. I. Bird, and S. Ulm. 2017. "Complexities in the Palaeoenvironmental and Archaeological Interpretation of Isotopic Analyses of the Mud Shell Geloina Erosa (Lightfoot, 1786)." *Journal of Archaeological Science: Reports* 12: 613–624. https://doi.org/10.1016/j.jasrep.2017.03.010.

Ulm, S., I. J. McNiven, S. J. Aird, and A. B. Lambrides. 2019. "Sustainable Harvesting of *Conomurex luhuanus* and *Rochia nilotica* by Indigenous Australians on the Great Barrier Reef Over the

Past 2000 Years." *Journal of Archaeological Science: Reports* 28: 102017. https://doi.org/10.1016/j.jasrep.2019.102017.

Ulm, S., I. J. McNiven, G. R. Summerhayes, et al. 2024. "Early Aboriginal Pottery Production and Offshore Island Occupation on Jiigurru (Lizard Island Group), Great Barrier Reef, Australia." *Quaternary Science Reviews*: 108624. https://doi.org/10.1016/j.quascirev.2024.108624.

von Leesen, G. 2014. "*Thin-Sections of Marine Bivalve Shells: A Window to Environmental Reconstructions on Daily Scale?*" Bachelor's thesis, University of Bremen.

Walliser, E. O., and B. R. Schöne. 2020. "Paleoceanography of the Late Cretaceous Northwestern Tethys Ocean: Seasonal Upwelling or Steady Thermocline?" *PLoS One* 15, no. 8: e0238040. https://doi.org/10.1371/journal.pone.0238040

Wanamaker, A. D., Jr., A. Baker, P. G. Butler, et al. 2009. "A Novel Method for Imaging Internal Growth Patterns in Marine Mollusks: A Fluorescence Case Study on the Aragonitic Shell of the Marine Bivalve *Arctica islandica* (Linnaeus)." *Limnology and Oceanography: Methods* 7, no. 9: 673–681. https://doi.org/10.4319/lom.2009.7.673.

Wang, T., D. Surge, and S. Mithen. 2012. "Seasonal Temperature Variability of the Neoglacial (3300–2500 BP) and Roman Warm Period (2500–1600 BP) Reconstructed From Oxygen Isotope Ratios of Limpet Shells (*Patella vulgata*), Northwest Scotland." *Palaeogeography, Palaeoclimatology, Palaeoecology* 317: 104–113. https://doi.org/10.1016/j.palaeo.2011.12.016.

Warner, J. P., K. L. DeLong, D. Chicoine, K. Thirumalai, and C. F. T. Andrus. 2022. "Investigating the Influence of Temperature and Seawater $\delta_{18}O$ on *Donax obesulus* (Reeve, 1854) Shell $\delta^{18}O$." *Chemical Geology* 588: 120638. https://doi.org/10.1016/j.chemgeo.2021.120638.

Welsh, K., M. Elliot, A. Tudhope, B. Ayling, and J. Chappell. 2011. "Giant Bivalves (*Tridacna gigas*) as Recorders of ENSO Variability." *Earth and Planetary Science Letters* 307, no. 3/4: 266–270. https://doi.org/10.1016/j.epsl.2011.05.032.

Yan, H., C. Liu, Z. An, et al. 2020. "Extreme Weather Events Recorded by Daily to Hourly Resolution Biogeochemical Proxies of Marine Giant Clam Shells." *Proceedings of the National Academy of Sciences* 117, no. 13: 7038–7043. https://doi.org/10.1073/pnas.1916784117.

Supporting Information

Additional Supporting Information may be found in the online version of this article.

Submitted 24 August 2025
Revised 22 December 2025
Accepted 05 January 2026